

Journal of Materials Chemistry A

Accepted Manuscript



This is an *Accepted Manuscript*, which has been through the Royal Society of Chemistry peer review process and has been accepted for publication.

Accepted Manuscripts are published online shortly after acceptance, before technical editing, formatting and proof reading. Using this free service, authors can make their results available to the community, in citable form, before we publish the edited article. We will replace this *Accepted Manuscript* with the edited and formatted *Advance Article* as soon as it is available.

You can find more information about *Accepted Manuscripts* in the [Information for Authors](#).

Please note that technical editing may introduce minor changes to the text and/or graphics, which may alter content. The journal's standard [Terms & Conditions](#) and the [Ethical guidelines](#) still apply. In no event shall the Royal Society of Chemistry be held responsible for any errors or omissions in this *Accepted Manuscript* or any consequences arising from the use of any information it contains.

Polyethyleneimine–Nano Silica Composites: A Low-Cost and Promising Adsorbent for CO₂ Capture

*Kaimn Li,^a Jianguo Jiang,^{*a,b,c} Sicong Tian,^a Feng Yan,^a Xuejing Chen^a*

^aSchool of Environment, Tsinghua University, Beijing 100084, P. R. China

^bKey Laboratory for Solid Waste Management and Environment Safety, Ministry of Education of China, P. R. China

^cCollaborative Innovation Center for Regional Environmental Quality, Tsinghua University, Beijing 100084, P. R. China

KEYWORDS: Carbon Capture, Amine-Silica adsorbent, Nano silica, CO₂ sorption, Polyethelenimine

ABSTRACT: Adsorbents for CO₂ capture with nano silica as support were synthesized by impregnating polyethyleneimine (PEI) into nano silica. For impregnation of PEI into nano silica, the pore of 2-40nm of silica support plays an important role in the synthesis process of adsorbents. The PEI loading content, adsorption temperature and CO₂ partial pressure influenced CO₂ adsorption capacity and PEI utilization efficiency. At 105°C, 60-wt% PEI loading content and 1atm CO₂ partial pressure, CO₂ adsorption capacity of 186 mg/g adsorbent and PEI utilization efficiency of 304 mg/g PEI were obtained. CO₂ cycling

adsorption–desorption test under the condition: adsorption at 90 or 105°C under pure CO₂ and desorption at 120°C under pure N₂ showed relatively good adsorption–desorption stability, and no obvious deactivation of amines was observed under this condition. However, under the condition: adsorption at 90 or 105°C under pure CO₂ and desorption at 135 or 150°C under pure CO₂, obvious deactivation of amines occurred and the formation of linear or cyclic urea led to the significantly decrease of CO₂ adsorption capacity.

INTRODUCTION

Scientists have stated that mankind must limit global average temperature rises to avoid potentially irreversible abrupt climate change. To be confident of achieving an equilibrium temperature increase of only 2 to 2.4°C, atmospheric greenhouse gas (GHG) concentrations must be stabilized at 445–490 ppm carbon dioxide (CO₂) atmospheric equivalents. Therefore, we must substantially reduce global CO₂ emissions no later than 2015. ^[1] According to the latest Greenhouse Gas Bulletin published by the World Meteorological Organization in 2013, the CO₂-equivalent concentration of the global atmosphere GHG reached 476 ppm in 2012, of which CO₂ alone constitutes 393 ppm. ^[2] Thus mankind is facing the challenge of reducing CO₂ emissions. In the current and coming decades, fossil fuels are and will remain mankind's primary energy source. ^[3] Therefore, we must accelerate development of efficient, energy saving, cost-effective, and easy-to-operate CO₂-capture technologies, and initiate the large-scale industrial application of such technologies.

At present, the 'aqueous solution of amines' technology has been used for CO₂ capture in industry, but has several disadvantages, such as high energy consumption, decomposition

of amines, and equipment corrosion.^[4] Therefore, solid adsorbents have attracted more attention as an alternative to ‘aqueous solution of amine’ technologies. Several solid adsorbents, such as zeolites,^[5, 6] activated carbon,^[7, 8] metal-organic frameworks (MOFs),^[9, 10] alkaline earth metal oxide,^[11, 12] and amine–silica hybrid/composited materials,^[13] have been investigated by many research groups. Of these solid adsorbents, zeolites, activated carbon, and MOFs need large pressure and/or temperature gradient to achieve good adsorption-desorption performance, furthermore the low selectivity to CO₂ and low tolerance to moisture also limit the use for CO₂ capture of them; ^[14] alkaline earth metal oxide generally require high temperature (650-850°C) to adsorb and desorb CO₂, ^[11] this will consume more energy and increase the difficulty of practical operation. Amine–silica hybrid/composite materials exhibit considerable adsorption capacity, low energy consumption, good selectivity to CO₂, good tolerance to moisture, and ease of handling, therefore Amine–silica hybrid/composite materials can be a good alternative to the ‘aqueous solution of amines’ technology.^[4, 14]

Amine–silica hybrid/composite materials are usually synthesized by grafting or impregnation. Both of these methods have merit; however, in terms of CO₂-adsorption capacity, impregnation seems superior to grafting. Builes and Vega ^[15] used Monte Carlo simulation to evaluate the influence of grafting and impregnation on the CO₂-capture behavior of amine–silica hybrid/composite materials. They found that impregnation consistently gave a higher adsorption capacity than grafting. Zhao *et al.* ^[16] synthesized two types of amine–silica hybrid by grafting and one type of amine–silica composite by impregnation; impregnation yielded a higher amine content and higher CO₂-adsorption

capacity than did grafting. Furthermore, Jones *et al.*^[17, 18] deemed the organic amine–silica composite adsorbents synthesized by impregnation to be the most practical adsorbents for large-scale gas separation applications in all kinds of amine-silica sorbents.

In recent years, many types of organic-amine have been used to impregnate various types of silica, such as nano silica (fumed silica, precipitated silica), silica gel, mesoporous silica (MCM-41, SBA-15), and so on, to capture CO₂. Olah *et al.*^[19] reported a very comprehensive research, they investigated 11 types of organic-amine and 9 types of support for synthesis of a series of adsorbents by impregnation, and a detailed analysis and comparison to each adsorbent was conducted. Branched low- and high-molecular-weight polyethyleneimines were particularly suitable for CO₂ capture due to their stability and high CO₂-capture capacity. Wang *et al.*^[20] and Jones *et al.*^[17] further pointed out that low-molecular-weight polyethyleneimine was superior to high-molecular-weight polyethyleneimine due to its higher primary amine content and greater mobility.

Olah *et al.*^[19] found that fumed silica and precipitated silica were better supports for impregnation than silica gel, aluminum oxide, poly (4-vinylpyridine), and povidone. And they also reported that mesoporous silica (MCM-41, SBA-15) was not necessary to achieve good CO₂ adsorption, and that precipitated or fumed silica yielded better results.^[19, 21] The CO₂ adsorption performance comparison for different PEI-silica composite sorbents with different type silica as matrix (Table 1) also support this. Of course, some other types of solid adsorbents, such as synthesized by impregnating PEI into MOFs also exhibit very good CO₂ adsorption performance,^[22] but MOFs is a complex support which the synthesis process is

much more complicated than nano silica, so this may limit its practical application in the future.

Impregnating polyethyleneimin into nano silica to synthesize CO₂ adsorbents (PEI-nano silica), it can exhibit high CO₂-adsorption capacities. Furthermore, PEI-nano silica adsorbents also show good adsorption–desorption cycle stability, as reported by Olah *et al.* [21] At present, the mesoporous silica synthesis method is complex and no commercial source of mesoporous silica on a large scale is available. [19] However, nano silica has been produced and used widely on a large scale for many years. This material is relatively cheap and easy to obtain. Therefore, nano silica can potentially decrease the cost of synthesis of amine–silica adsorbents. For this reason, PEI-nano silica adsorbents may be a good choice for future application in flue gas separation. However, to our knowledge, research on PEI-nano silica adsorbents is not enough and further research is need to be done.

In our study, a series of PEI-nano silica adsorbents with various PEI loading contents were synthesized. The relationship between the pore volume chang of nano silica and PEI-loaded content, and the thermal stability of PEI-nano silica adsorbents, were assessed. The influence of temperature, PEI loading content and CO₂ partial pressure on the CO₂-adsorption capacity of PEI-nano silica adsorbents, and the adsorption–desorption cycle stability of PEI-nano silica under different conditions was investigated, and the reason caused the decrease of CO₂ cycle adsorption-desorption stability of PEI-nano silica sorbents was analyzed.

EXPERIMENTAL

Reagents

Nano silica (precipitated silica, Sipernant 306) was obtained from Evonik (Germany). Polyethyleneimine (branched, M.W. 600, 99%, 1.03 g/cm³) was purchased from Alfa Aesar (United States). Methanol (HPLC grade) was purchased from Fisher (United States). CO₂ gas (99.999%), 15% CO₂ with N₂ as balance gas, N₂ (99.999%) was purchased from ZG Special Gases (Beijing, China).

Preparation of PEI-nano silica adsorbents

First, the desired amount of PEI was dissolved in 25-ml methanol under stirring with a magnetic stirrer. After the PEI had dissolved completely, 2-g nano silica (dried for 2 h under 110°C and vacuum [<1 mm Hg]) was then added, and 5-ml methanol was subsequently added to the solution. Thereafter, the solution was stirred at room temperature (~ 8 h at 25°C) until it became sticky. Subsequently, the product was dried for 3 h at 50°C, and again for 2 h at 50°C under vacuum (<1 mm Hg). The materials were termed *x*-PEI-Silica; *x* refers to the theoretical content of PEI of the materials, and the actual PEI content of the materials determined by elemental analysis is shown in Table S1.

Elemental analysis

C, H, and N elemental contents were determined using an EA 3000 elemental analyzer (Euro Vector) with the following accuracies: C $\leq \pm 0.10\%$, H $\leq \pm 0.10\%$, and N $\leq \pm 0.05\%$. For each material, three parallel samples were used for analysis; the weight of each was controlled to within 1–2 mg.

Thermal stability analysis

Thermal stability analysis of PEI-nano silica adsorbents was conducted using a TGA/DSC 1 STAR^e thermogravimetric analyzer (Mettler Toledo). The test started at 30°C and ended at 800°C at a heating rate of 10°C/min under an N₂ atmosphere with a flow rate of 20 ml/min. 5–10-mg sample was placed into an aluminum pan for analysis.

N₂ adsorption–desorption analysis

N₂ adsorption-desorption analysis was performed using an ASAP 2020 analyzer (Micromeritics). The degassing process for plain nano silica involved maintaining pressure in the sample tube at less than 100 μm Hg for 3 h at 110°C. For PEI-nano silica adsorbents, the pressure in the sample tube was maintained at less than 100 μm Hg for 8 h at 50°C. Analysis of all materials was conducted at -196°C. The surface area was calculated using a Brunauer–Emmett–Teller (BET) model, and the pore distribution was calculated using a Barrett–Joyner–Halenda (BJH) model. The total pore volume was estimated at a relative pressure of 0.99.

CO₂ adsorption analysis

CO₂ adsorption analysis was performed using a Q500 thermogravimetric analyzer (TA Instruments). Firstly, material was pretreated for 30 min at 120°C under N₂ at a flow rate 90 ml/min. The temperature was then decreased to the test temperature (45, 60, 75, 95, or 105°C). After being maintained for 10 min isothermally at the tested temperature, the N₂ was switched to pure CO₂ for 60 min.

The cycle analysis under condition 1 (adsorption at 90 or 105°C under a pure CO₂ atmosphere and desorption at 120°C under an N₂ atmosphere) was performed using a Q500 thermogravimetric analyzer (TA Instruments), and under condition 2 (adsorption at 90 or 105°C under a pure CO₂ atmosphere and desorption at 135 or 150°C under a pure CO₂ atmosphere) was performed using a TGA/DSC 1 thermogravimetric analyzer (Mettler Toledo).

FTIR analysis

Fourier-transform infrared spectroscopy (FTIR) analysis was performed using a Thermal NEXUS spectrometer (Thermo Scientific) with an 8 cm⁻¹ resolution and 32 min⁻¹ scanning frequency at room temperature. The spectra were recorded in the 4000–400-cm⁻¹ region.

RESULTS AND DISCUSSION

N₂ adsorption–desorption analysis

The pore distributions of plain silica and PEI-silica materials, calculated from the N₂ adsorption–desorption isotherms (Figure S1), are shown in Figure 1. Here, to show more clearly the change in the pore distribution of silica after impregnation, a mathematical manipulation of the unit of pore volume (*y*-axis) is shown in Figure 1. In the original data provided by measurement instruments, the unit of pore volume was per gram adsorbent (composite of silica and PEI) as the denominator (Figure S2). However, this cannot clearly demonstrate the change in the silica pore distribution, so altered the denominator to 1 g of silica by mathematical manipulation.

Impregnation of PEI alters the silica pore distribution (Figure 1). With PEI-content increase, the total pore volume of silica decreased markedly (Table S2) and the pore volume of mesopore (2-50nm) decrease obviously; however, at a relatively small pore size, the silica pore volume increased after impregnation compared with plain silica. For example, pores were ≤ 5.0 nm in silica with 10% PEI, ≤ 4.4 nm with 20% PEI, ≤ 3.3 nm with 30% PEI, ≤ 2.8 nm with 35% PEI, and ≤ 2.6 nm with 40% PEI. In silica impregnated with 50% and 60% PEI, the pore volume at all pore size ranges exhibited an overall decline, with the exception of pores ≤ 2.3 nm in silica impregnated with 50% PEI; this is a distribution similar to that of plain silica.

The pore distribution change in silica with various PEI contents can be explained in the following two ways: (1) During the impregnation process, PEI diffuses into the pores under capillary pressure and concentration difference force; ^[29-32] meanwhile, the PEI molecule is adsorbed onto the silica pore walls. ^[32-34] Along with the increase of PEI content, the adsorption layer of PEI onto the silica surface will also thicken, ^[35, 36] so this will lead to gradual decreases in pore size and volume, and some relative large pore become small size pore, for example the pore of 3nm become the pore of 1.8nm. (2) As the PEI loading content increases, so does the probability of pore blockage, leading to some pores being inaccessible to N₂ adsorption, and this will lead to the decrease of the pore volume. ^[34, 37]

In Figure 1, the most obvious changes of the pore volume happens in the mesopore range (2-50nm), especially in the range 2-40nm with the PEI content increase when the PEI contents $\leq 50\%$. Due to the total pore volume of the plain silica is 1.28 cm³/g, this means the

highest PEI loading content can only be reached 57% in theory, so when the PEI content reaches 60% some PEI molecules will locate the outside surface of the silica supports, the SEM images (Figure S4) can better supports this. So in figure 2 and figure S3, the pore volume loss in different pore range was not be used to analyze the relationship between the pore volume loss and the PEI loading content. The figure 2 and the figure S3 show that the pore volume loss in the range 2-40nm with the PEI loading content fits better ($R^2=0.9924$) than that of between the pore volume loss in the other pore range (2-20, 30, 50, 60, 70, 80, and 100nm) and the PEI loading content, this indicated that the pore of 2-40nm had an important role in the PEI impregnation process.

For the average pore diameter, an interesting phenomenon was observed, the average pore diameter increase with PEI content increase until the PEI content reaches 50%, and then diving when the PEI content reaches 60% (Table S2). For this phenomenon, it most likely due to that the PEI molecules prefer to diffuse into small size pores of silica, this leads to the blockage of the small size pores and large size pores are remained, therefore on one side the total pore volume decrease and on the other side the average pore diameter will increase. However, when the volume of loading PEI volume excess 1.28cm^3 (the total pore volume of plain silica) in 1 g silica, the serious pore blockage will happen and the average pore diameter will decrease obvious, just as 60% PEI-silica sorbent shows. The TEM images (Figure S3) for plain silica, 30% PEI-silica, and 60% PEI-silica can give some information to support this.

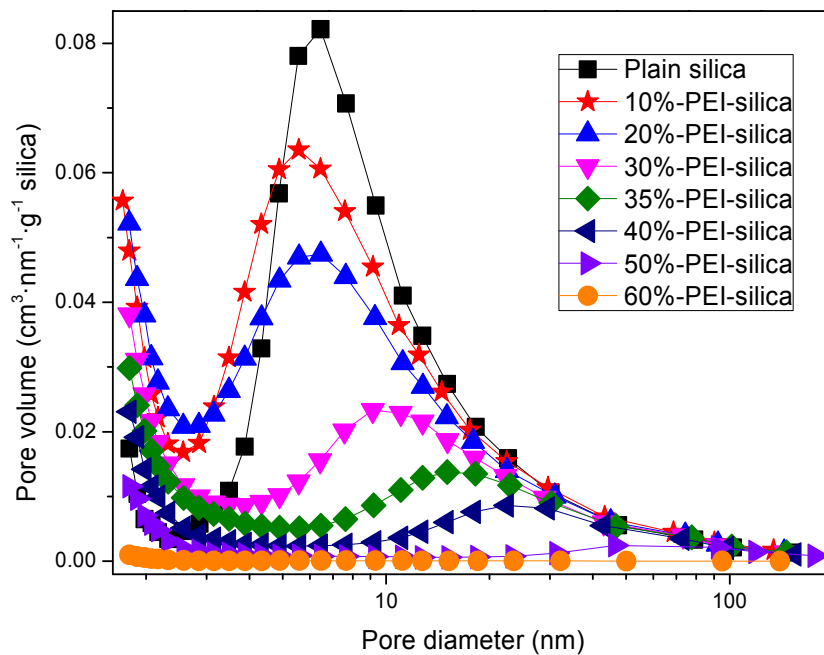


Figure 1. Pore distributions of plain silica and PEI-nano silica adsorbents with different PEI content.

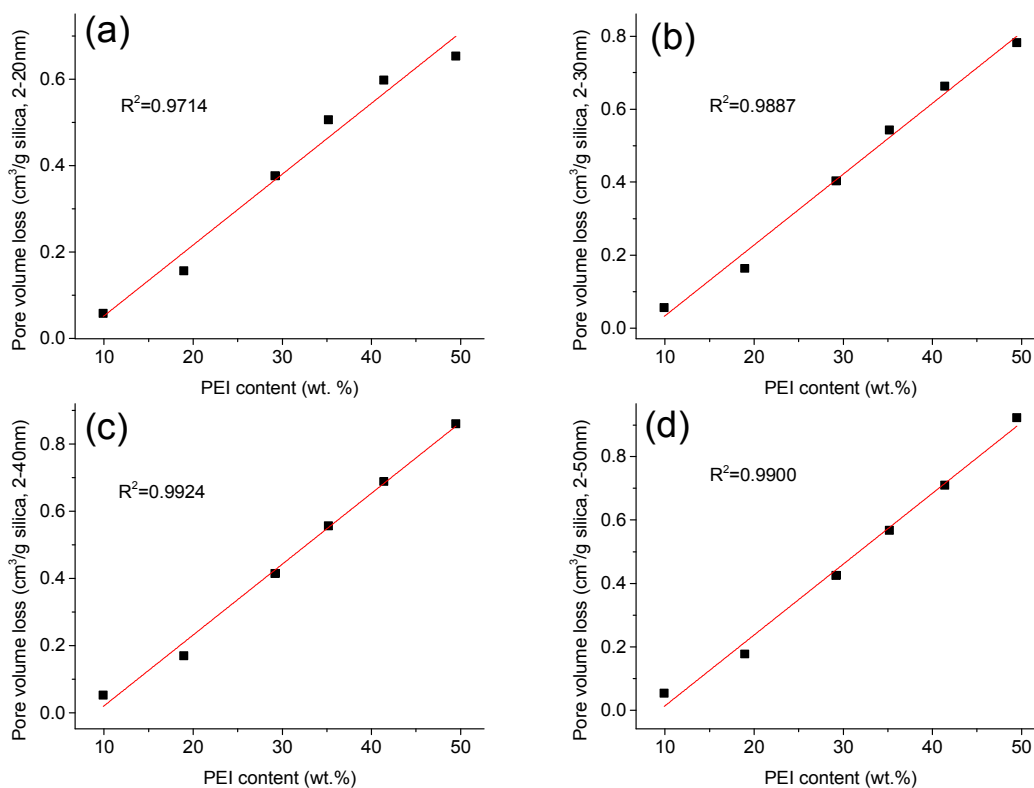


Figure 2. The relationship between the PEI loading content and the pore volume loss in the range: (a) 2-20nm, (b) 2-30nm, (c) 2-40nm, (d) 2-50nm.

Thermal stability analysis

Results of thermo-gravimetric analysis of plain silica, PEI-silica adsorbents with various PEI contents, and pure PEI, are shown in Figure 2. The differential curve of weight to temperature clearly indicates two weight-loss stages for PEI-silica adsorbents. From 30 to 135°C, the weight loss of PEI-silica adsorbents is due mainly to the release of physically and chemically adsorbed water.^[38, 39] From 165 to 500°C, the rapid weight loss is attributable mainly to the volatilization and decomposition of PEI molecules. The de-hydroxylation of silica also contributes to the weight loss of PEI-silica adsorbents from 165 to 500°C.^[40]

The differential curves of weight to temperature suggest a bimodal model between 165 and 500°C for 35%-PEI-silica, 40%-PEI-silica, and 50%-PEI-silica adsorbents. This phenomenon is caused mainly by the distribution of PEI molecules in the silica pores. The former peak is the volatilization and decomposition of PEI molecules located in the shallower parts of the pores and the outside surface of the silica, and the latter peak indicates the volatilization and decomposition of PEI molecules located in the deeper parts of the pores.^[41] However, for 10, 20, 30, and 60%-PEI-silica adsorbents, only one peak was observed. When the PEI content was $\leq 30\%$, the PEI molecules occur mainly relatively deep in the silica pores; thus all PEI molecules were located in a similar environment. Therefore, during the heating process the volatilization and decomposition of the vast majority of PEI molecules is synchronized so that only one peak results.

With increasing PEI content, two classes of PEI molecules form in two different environments. Therefore, during the heating process, the volatilization and decomposition of PEI molecules will be asynchronous, and, therefore, two peaks will appear, as shown by 35, 40, and 50%-PEI-silica. At a PEI content of 60%, the PEI molecules located in the shallow regions and the outside surface of the silica occupy the largest area, so the former peak will mask the latter and a single peak will again be observed.

Thermo-gravimetric analysis indicated that the PEI-silica adsorbents exhibited relatively good thermal stability below 160°C. Volatilization of a minimal number of PEI molecules occurs below 160°C. A more detailed thermo-gravimetric analysis of 60% PEI-silica adsorbents (Figure S4) showed that from 30° to 200°C at a slow heating rate (2°C/min), the weight loss occurred mainly below 100°C; and between 100 and 160°C, the weight loss, which was most likely caused by the volatilization of relatively small PEI molecules, was ~6.5%.

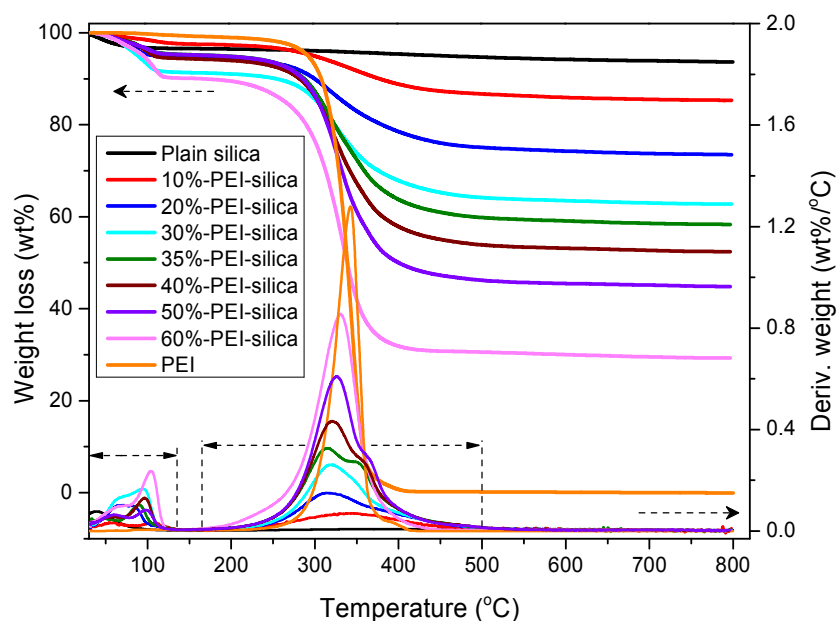


Figure 3. Thermo-gravimetric analysis of plain silica, PEI–silica adsorbents, and pure PEI.

CO₂ adsorption analysis

CO₂ adsorption capacity of PEI-nano silica adsorbents at 45, 60, 75, 90, and 105°C is shown in Figures 3 and 4. Figure 3 shows the influence of temperature, and Figure 4 shows that of PEI loading content.

A similar variation in adsorption capacity to all adsorbents is evident in Figures 3a and b. The 10, and 20% PEI-silica exhibited a clear downtrend with increasing temperature. With regard to 30% PEI-silica, from 45 to 60°C adsorption capacity increased by ~2.3%, but above 60°C, the adsorption capacity decreased with increasing temperature. At PEI content of 35–50%, the adsorption capacity increased with temperature increase when the temperature is $\leq 90^\circ\text{C}$, and a decrease occurs from 90 to 105°C. The adsorption capacity of 60%-PEI-silica adsorbent increased from 45 to 105°C almost in a linear fashion.

Temperature has two effects on the CO₂-adsorption capacity of PEI-nano silica adsorbents: (1) a reduction effect (the thermal effect) due to the reaction of CO₂ and amines, an exothermic process by which the adsorption capacity decreases with increasing temperature. [42–44] (2) An increasing effect (the mobility effect), in which increasing temperature enhances the mobility of PEI molecules in PEI-nano silica adsorbents, potentially leading to an increased adsorption capacity. [42, 45] However, the roles of the two effects vary under different conditions. At PEI contents $\leq 30\%$, the thermal effect is dominant. However, at PEI contents of 35–50%, the mobility effect dominates up to 90°C. At 105°C, the thermal effect increases obviously. At a PEI content of 60%, the mobility effect dominates from 45 to 105°C.

The adsorption capacity of PEI-silica adsorbents first increases, then decreases with increasing PEI content, except at 90–105°C (Figure 4a). In addition, at a PEI content $\leq 35\%$, the adsorption capacity increases rapidly with increasing PEI content. However, at PEI contents $> 35\%$, the increase in adsorption capacity slows and begins to decrease at PEI contents $\geq 60\%$. At 90–105°C, the CO₂-adsorption capacity increased with increasing PEI content; although, the CO₂-adsorption capacity increases only 3% PEI contents increased from 50% to 60% at 90°C.

An initial increase, followed by a decrease, with increasing PEI contents was observed in Figure 4b. One possible reason for this phenomenon is that with increasing PEI contents, the proportion of PEI molecules located in the shallow portions of the pores and outside surface of the silica increases. Molecules in these locations can better interact with CO₂ and

therefore exhibit greater PEI utilization efficiency. However, at a threshold PEI content, the polymerization of PEI molecules and pore blocking will begin to dominate, leading to a decreased PEI utilization efficiency.

PEI-loading content also affects the adsorption capacity of PEI-silica adsorbents in two respects: (1) increasing PEI content leads to an increased amine content, potentially increasing the number of CO₂ capture sites. (2) The increase in PEI content also will lead to pore blockage of adsorbent and aggregation of PEI molecules, reducing the opportunities for CO₂ capture of some amine; but this effect has something with property of silica support and temperature, furthermore only when the PEI content reaches a certain degree it will do obviously; figure 4a clearly shows that only when the PEI content reaches 60% and the temperature doesn't exceed 75°C, it will work obviously.

Therefore, the adsorption capacity of PEI-silica adsorbents is influenced by the temperature and PEI-loading content under pure CO₂. This can be described by the function: $Y = f(T, C)$, in which T and C refer to the adsorption temperature and PEI-loading content, respectively; Y refers to the adsorption capacity, expressed as mg CO₂/g adsorbent or mg CO₂/g PEI. When using mg CO₂/g PEI as the unit of adsorption, Y also refers to the PEI utilization efficiency. The highest CO₂-adsorption capacity (186 mg/g adsorbent) is attained at $T = 105^{\circ}\text{C}$ and $C = 60\%$. Moreover, under this condition, the PEI utilization efficiency is 304 mg/g PEI. Although $f(90, 60\%) = 165$ mg/g adsorbent and is only after $f(105, 60\%)$, the PEI utilization efficiency is only 268 mg/g PEI. All adsorption amounts under all conditions are not listed here; this information is provided in Table S3 and S4.

In order to better learn the CO₂ adsorption performance of PEI-nano silica adsorbents, and considering that the real flue gas generally contains 15% CO₂, so the CO₂ adsorption performance under 0.15atm CO₂ partial pressure (with N₂ as balance gas) at 75°C is investigated (Figure S7). The results show that the saturated CO₂ adsorption capacity of 10%-PEI-silica, 20%-PEI-silica, 30%-PEI-silica, 35%-PEI-silica, 40%-PEI-silica, 50%-PEI-silica, 60%-PEI-silica are 8, 37, 77, 98, 109, 134, 132mg/g respectively under 0.15atm CO₂ partial pressure which are lower than that under pure CO₂ (Table S3). So for PEI-nano silica adsorbents, the CO₂ partial pressure also influence the saturated CO₂ adsorption capacity. Therefore the CO₂ adsorption capacity of PEI-nano silica adsorbents can be depicted as function $Y = f(T, C, P)$, in which T , C , and P refer to the adsorption temperature, PEI-loading content, and CO₂ partial pressure respectively.

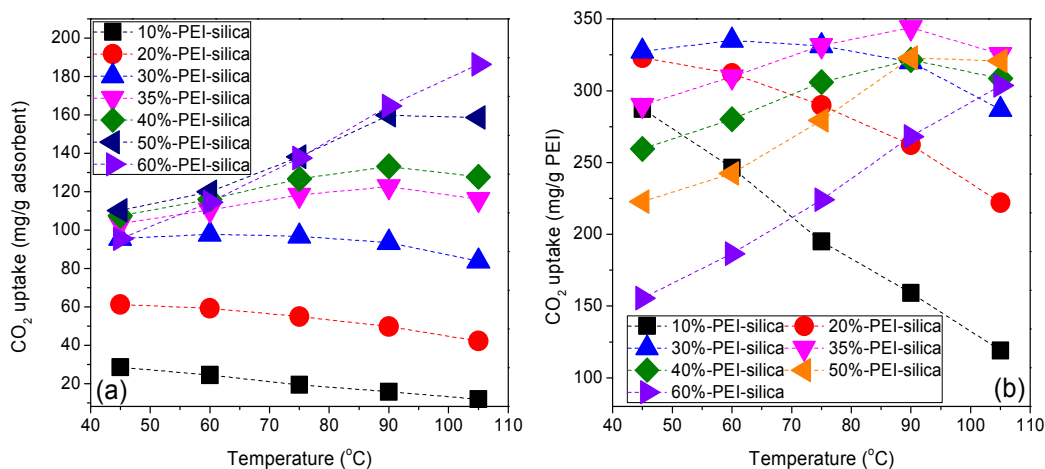


Figure 3. Effect of temperature on CO₂ adsorption analysis of PEI-silica adsorbents.

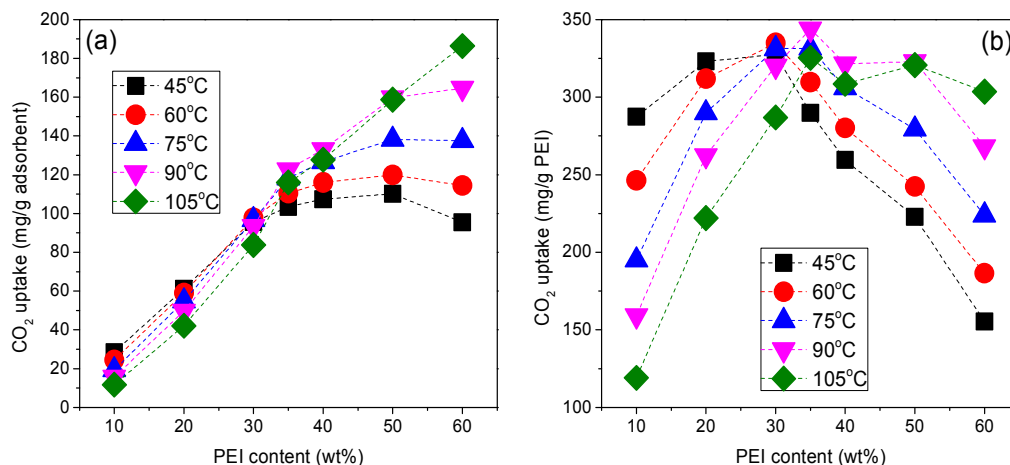


Figure 4. Effect of PEI loading content on CO₂ adsorption analysis of PEI-silica adsorbents.

Table 1. Comparison of all kinds PEI-silica composite CO₂ adsorbents.

Sorbent	Silica	PEI type ^a	PEI content (wt %)	CO ₂ pressure	Temp. (°C)	Sorption capacity (mg /g)	Ref.
Si-MCM-41-PEI-50-S8	MCM-41	—	50%	1bar	75	126	23
Silica Gel-PEI-50	Silica gel	—	50%	1 bar	75	78	23
MCM-41-PEI-75	MCM-41	—	75%	1 bar	75	133	24
MCM-41-PEI-50	MCM-41	—	50%	1 bar	50	44	24
MCM-41-PEI-50	MCM-41	—	50%	1 bar	75	112	24
MCM-41-PEI-50	MCM-41	—	50%	1 bar	100	110	24
SBA-15-PEI (50)	SBA-15	B800	50%	1 bar	75	89.8	25
SBA-15-PEI (50)	SBA-15	B800	50%	5.5 bar	75	95.4	25
I-SBA-15-PEI-50	SBA-15	B800	50%	0.15 bar	45	71.2	26
I-SBA-15-PEI-50	SBA-15	B800	50%	1 bar	45	74.6	26
I-SBA-15-PEI-50	SBA-15	B800	50%	4.5bar	45	80.3	26
Prec. SiO ₂ /PEI (1:1)	Precipitated silica	B800	50%	1bar	70	147	19
Prec. SiO ₂ /PEI (1:1)	Precipitated silica	B800	50%	1bar	85	160	19
Fumed SiO ₂ /PEI (1:1)	Fumed silica	B800	50%	1bar	85	156	19
Prec. SiO ₂ /PEI (1:1)	Precipitated silica	L423	50%	1bar	70	173	19
50wt% PEI/SBA-15	SBA-15	L423	50%	1bar	75	173	20
MCM-41-PEI-50	MCM-41	L600	50%	1bar	75	111	27
SBA-15-PEI-50	SBA-15	L600	50%	1bar	75	127	27
SBA-16-PEI-50	SBA-16	L600	50%	1bar	75	129	27

MCM-48-PEI-50	MCM-48	L600	50%	1bar	75	119	27
KIT-6-PEI-50	KIT-6	L600	50%	1bar	75	135	27
50PEI/B-T100	Silica derived from rice husk ash	-	50%	1bar	90	149	28
60PEI/B-T100	Silica derived from rice husk ash	-	60%	1bar	90	154	28
A-PEI-300	MIL-101 (Cr, 150nm)	L300	50%	0.15bar	50	158	22
B-PEI-300	MIL-101 (Cr, 250nm)	L300	50%	0.15bar	50	180	22
50%-PEI-silica	Precipitated silica	B600	50%	0.15bar	75	134	This study
60%-PEI-silica	Precipitated silica	B600	60%	0.15bar	75	132	This study
50%-PEI-silica	Precipitated silica	B600	50%	1bar	75	138	This study
60%-PEI-silica	Precipitated silica	B600	60%	1bar	75	137	This study
50%-PEI-silica	Precipitated silica	B600	50%	1bar	90	160	This study
60%-PEI-silica	Precipitated silica	B600	60%	1bar	90	165	This study
60%-PEI-silica	Precipitated silica	B600	60%	1bar	105	186	This study

^a B means branched PEI and L means linear PEI.

CO₂ cycling adsorption–desorption analysis

Evaluation of CO₂ cycling adsorption–desorption for 30 cycles under various conditions is shown in Figures 5 and 6. Figure 5 shows the results under condition 1: adsorption at 90 or 105°C under pure CO₂ and desorption at 120°C under pure N₂. Figure 6 shows the results under condition 2: adsorption at 90 or 105°C and desorption at 120, 135 or 150°C under pure CO₂ without a gas change. We define the adsorbents after cycling as adsorbent– x/y –N₂ or CO₂, in which x and y represent the adsorption and desorption temperatures, respectively, N₂ or CO₂ refers to the desorption atmosphere. For example, 35%-PEI-silica-90/120-N₂ is a

cycling adsorption–desorption test at 90°C for adsorption and 120°C for desorption under pure N₂.

After 30 rounds in the cycling adsorption–desorption test, all adsorbents exhibited a more or less decrease in CO₂-adsorption capacity. However, the cycling adsorption–desorption stability of PEI-nano silica adsorbents under the two conditions differs considerably. Under condition 1, the adsorption–desorption stability of adsorbents was superior to that under condition 2. For 35%-PEI-silica-90/120-N₂, 40%-PEI-silica-90/120-N₂, 50%-PEI-silica-90/120-N₂, 60%-PEI-silica-90/120-N₂, and 60%-PEI-silica-105/120-N₂, the adsorption capacity decreased by 10.4%, 10.1%, 7.7%, 6.9%, and 10.5%, respectively. However, under condition 2, for 50%-PEI-silica-90/135-CO₂, 50%-PEI-silica-90/150-CO₂, and 60%-PEI-silica-105/150-CO₂, the adsorption capacity decreased by 79.8%, 91.9%, and 94.7%, respectively.

For condition 1, the FTIR spectra of fresh adsorbents and adsorbents after 30 cycles were identical, and no new bands are evident for adsorbents after 30 cycles. For example, Si–O–Si stretching or bending vibration (~469, 813, and 1101 cm⁻¹), ^[46] C–H stretching vibration (~2825 cm⁻¹), ^[42] N–H bending vibration (~1570 cm⁻¹), ^[46] –CH₂– bending vibration (~1469 and 2939 cm⁻¹), ^[47] or OH vibration (center at ~3418 cm⁻¹) ^[46, 48] may be responsible. No clear deactivation of amines was found ^[14, 50] for the PEI-nano silica adsorbents after 30 cycles adsorption-desorption test under condition 1. However, for condition 2 the FTIR spectral results of fresh and the adsorbents after 30 cycles adsorption–desorption test differed significantly. Four obvious new bands, at ~1277, 1454, 1496, and

1693 cm^{-1} , which are not present in the spectra of the fresh adsorbents, are evident in the spectra of adsorbents after 30 adsorption–desorption cycles under condition 2. These new bands are strongly associated with the formation of linear or cyclic ureas.^[14, 50] The new band at 1693 cm^{-1} also can be observed in the IR spectrum of fresh carbamide, and this band most likely be the vibration of C=O. So under condition 2, the degradation of amines is a reason caused the decrease of CO_2 adsorption capacity.^[50]

Besides the degradation of amines, the volatilization^[49] and leaching^[19] of PEI are another two main reasons cause the decrease of CO_2 adsorption capacity of PEI-nano silica sorbent. Because the molecular weight of PEI is not uniform, some relatively light molecules are present in bulk PEI; and these are readily volatilized, which leads to the loss of PEI. The C, H, and N elemental analyses (Table 1) show that after 30 cycles the PEI content decreases compared with fresh adsorbents. With temperature increase and reach a certain level, the mobility of amines obviously increase and this will lead to the leaching of amine from the silica pores, the CO_2 capture ability of leaching amine will obvious decrease. To our knowledge, at present there is no method and theory to quantificationally analyze the leaching level of amines, but we think the leaching level of amies is influenced by temperature, and the leaching level of amines increase with temperature increase.

Under condition 1, the decrease in CO_2 -adsorption capacity is attributable mainly to the volatilization and leaching of PEI. For condition 2, formation of urea, volatilization of PEI and leaching of PEI together cause the decrease of CO_2 capacity. Under condition 2, the volatilization amount of PEI (Table 2) can not lead to the CO_2 adsorption capacity decrease

more than 80%, so the degradation of amines by forming urea and leaching of amine are the main reason causing the decrease of CO₂ adsorption. In figure 6, the cycling adsorption-desorption test for 50% PEI-silica under three different desorption temperature (120, 135, and 150°C) exhibits different cycling adsorption-desorption stability, this most likely due to that temperature influence the formation of urea and the leaching level of amines.

Changing the temperature and gas atmosphere (desorption under N₂), as in condition 1, is a commonly used method of achieving CO₂ desorption in much research. Although this method results in a high desorption capacity, it may not be suitable for practical industrial applications because this method must increase the subsequent gas separation process after desorption to again separate CO₂ from the mixing gas. Therefore, investigating CO₂ desorption by changing the temperature but not the gas (under pure CO₂) is meaningful and has practical implications. However, our data suggest a considerable decrease in CO₂-adsorption capacity under condition 2 for the PEI-nano silica adsorbents due to urea formation and leaching of amines. Therefore, further research is needed, for example the influence of water vapor on the cycle adsorption-desorption stability, pressure swing adsorption (PSA).

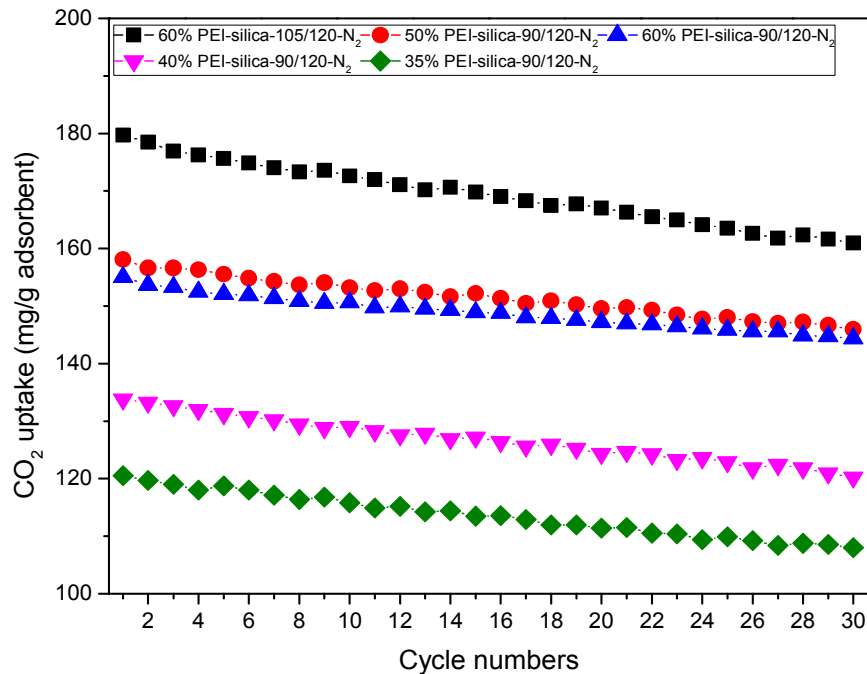


Figure 5. CO₂ cycle adsorption–desorption analysis under condition 1.

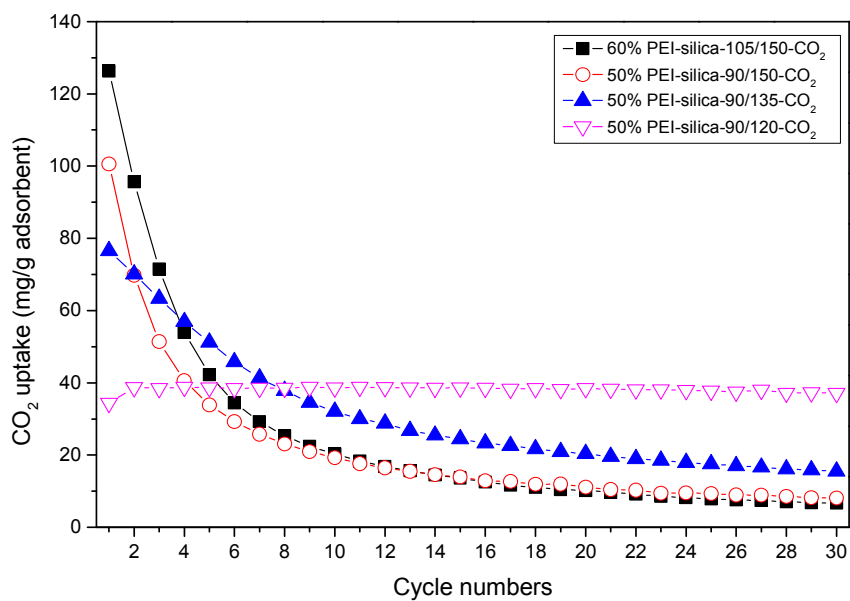


Figure 6. CO₂ cycle adsorption–desorption analysis under condition 2.

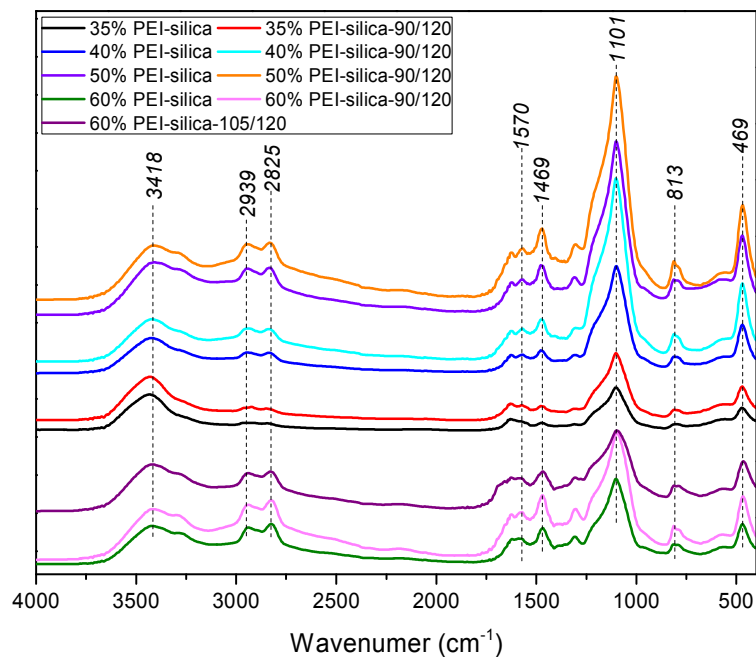


Figure 7. FTIR analysis of fresh PEI-silica adsorbents and adsorbents after 30-cycle adsorption–desorption under condition 1.

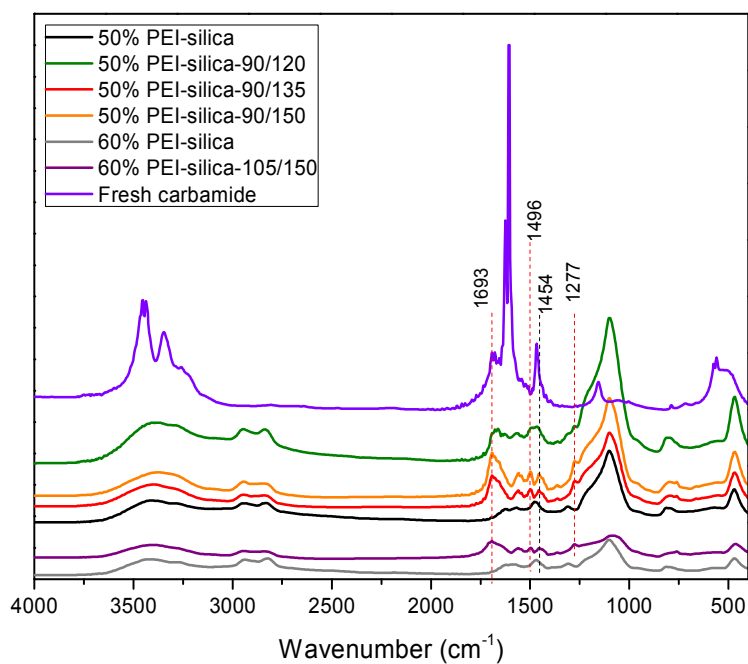


Figure 8. FTIR analysis of fresh PEI-silica adsorbents and adsorbents after 30-cycle adsorption–desorption under condition 2.

Table 2. C, H, and N elemental analysis of fresh adsorbents and adsorbents after 30 adsorption–desorption cycles under condition 2.

Sample	Elemental content (%)			PEI content (%)
	C	H	N	
50% PEI-silica	27.39	5.92	16.15	49.46 ^a
50% PEI-silica-90/135	28.50	4.32	15.10	46.25 ^b
50% PEI-silica-90/150	28.66	4.05	15.01	45.98 ^b
60% PEI-silica	34.14	7.26	19.98	61.38 ^a
60% PEI-silica-105/150	35.93	5.14	18.91	58.10 ^b

^a The PEI content is the result of the sum of C, H, and N content, which have deducted the C, H, and N content of plain silica.

^b The PEI content is calculated by the following formula: PEI content = N content of materials after 30 cycles/(N content of fresh materials/PEI content of fresh materials); here, we hypothesize that the N content of PEI in the materials is constant after 30 cycles.

CONCLUSIONS

With nano silica as support to synthesize amine-silica adsorbents for CO₂ capture can potentially decrease the cost of CO₂ adsorbents. In our study, we impregnated PEI into nano silica to synthesize PEI-nano silica adsorbents for CO₂ capture. Both PEI loading content and adsorption temperature influenced the CO₂ adsorption capacity. With PEI content increase, on one hand, more CO₂ capture sites will be supplied; on the other hand, the porosity of adsorbents will decrease and influence the diffusion of CO₂. The higher temperature can increase the mobility of PEI molecules and overcome the impact of pore blockage. The adsorbent contained 60-wt% PEI obtained a capture capacity of 186 mg/g at 105°C under pure CO₂, and the PEI utilization efficiency also reached 304 mg/g PEI. We think that a relatively good balance between PEI loading content and adsorption temperature can be obtained for PEI-nano silica adsorbents at the

condition: impregnating 60-wt% PEI and adsorption at 105°C. The cycling adsorption–desorption tests under the two different conditions (Experimental part) showed that the adsorption–desorption stability under the condition 2 is much worse than that under condition 1. For condition 1, the decrease of CO₂ adsorption capacity was due mainly to the loss of low-molecular-weight PEI molecules; for condition 2, the decrease of CO₂ adsorption capacity was due mainly to the formation of linear or cyclic urea. Compared the two conditions, we also found that temperature seems to be an important factor for the formation of urea under pure CO₂; higher temperature seems to be necessary to lead to the formation of urea under pure CO₂.

ASSOCIATED CONTENT

Supporting Information

The experimental protocol, and C, H, and N elemental analysis results can be found in Table S1 in supporting information. The N₂ adsorption–desorption isotherms and pore distributions of plain silica and PEI-nano silica adsorbents are shown in Figure S1 and S2, respectively. TEM images for plain silica, 30% PEI-silica, and 60% PEI-silica are showed in figure S3. BET area, total pore volume and average pore diameter data of plain silica and PEI-nano silica adsorbents can be found in Table S2. The CO₂ adsorption capacity of PEI-nano silica adsorbents is summarized in Table S3 and S4.

AUTHOR INFORMATION

Corresponding Author

* E-mail: jianguoj@tsinghua.edu.cn.

ACKNOWLEDGMENT

This work is supported by the Ministry of Science and Technology of the People's Republic of China (National 863 Program, Project NO. 2012AA06A116).

REFERENCES

- (1) Working Group III of the IPCC, Renewable Energy Sources and Climate Change Mitigation: Summary for Policymakers and Technical Summary. *Intergovernmental Panel on Climate Change* **2011**.
- (2) World Meteorological Organization, Greenhouse Gas Bulletin: The State of Greenhouse Gases in the Atmosphere Based on Global Observation through 2012. **2013**.
- (3) U.S. Department of Energy, International Energy Outlook 2013 with Projections to 2014. Washington, D.C., **2013**.
- (4) Sun, Z.; Fan, M.; Argyle, M. Supported Monoethanolamine for CO₂ Separation. *Ind. Eng. Chem. Res.* **2011**, *50*, 11343–11349.
- (5) Miyamoto, M.; Fujioka, Y.; Yogo, K. Pure Silica CHA Type Zeolite for CO₂ Separation Using Pressure Swing Adsorption at High Pressure. *J. Mater. Chem.* **2012**, *22*, 20186-20189.
- (6) Bae, T.-H.; Hudson, M. R.; Mason, J. A.; Queen, W. L.; Dutton, J. J.; Sumida, K.; Micklash, K. J.; Kaye, S. S.; Brown, C. M.; Long, J. R. Evaluation of Cation-Exchange Zeolite Adsorbents for Post-combustion Carbon Dioxide Capture. *Energy Environ. Sci.* **2013**, *6*, 128-138.
- (7) Xing, W.; Liu, C.; Zhou, Z.Y.; Zhang, L.; Zhou, J.; Zhuo, S. P.; Yan, Z. F.; Gao, H.; Wang, G. Q.; Qiao, S. Z. Superior CO₂ Uptake of N-Doped Activated Carbon Through Hydrogen-Bonding Interaction. *Energy Environ. Sci.* **2012**, *5*, 7323-7327.

- (8) Sevilla, M.; Fuertes, A. B.; Sustainable Porous Carbons with a Superior Performance for CO₂ Capture. *Energy Environ. Sci.* **2011**, *4*, 1765-1771.
- (9) Zhang, Z. J.; Yao, Z. Z.; Xiang, S. C.; Chen, B. L. Perspective of Microporous Metal-Organic Frameworks for CO₂ Capture and Separation. *Energy, Environ. Sci.* **2014**, *7*, 2868-2899.
- (10) Xu, Q.; Liu, D. H.; Yang, Q. Y.; Zhong, C. L.; Mi, J. G. Li-Modified Metal-Organic Frameworks For CO₂/CH₄ Separation: a Route to Achieving High Adsorption Selectivity. *J. Mater. Chem.* **2010**, *20*, 706-714.
- (11) Valverde, J. M. Ca-Based Synthetic Materials with Enhanced CO₂ Capture Efficiency. *J. Mater. Chem. A* **2013**, *1*, 447-468.
- (12) Gao, Y. S.; Zhang, Z.; Wu, J. W.; Yi, X. F.; Zheng, A.; Umar, A.; O'Hare, D.; Wang, Q. Comprehensive Investigation of CO₂ Adsorption on Ma-Al-CO₃ LDH-Derived Mixed Metal oxides. *J. Mater. Chem. A* **2013**, *1*, 12782-12790.
- (13) Boot-Handford, M. E.; Abanades, J. C.; Anthony, E. J.; Blent, M. J.; Brandani, S.; Dowell, N. M.; Fernández, J. R.; Ferrari, M.-C.; Gross, R.; Hallett, J. P.; Haszeldine, R. S.; Heptonstall, P.; Lyngfelt, A.; Makuch, Z.; Mangno, E.; Poter, R. T. J.; Pourkashanian, M.; Rochelle, G. T.; Shah, N.; Yao, J. G.; Fennell, P.S. Carbon Capture and Storage Update. *Energy, Environ. Sci.* **2014**, *7*, 130-189.
- (14) Sayari, A.; Belmabkhout, Y. Stabilization of Amine-Containing CO₂ Adsorbents: Dramatic Effect of Water Vapor. *J. Am. Chem. Soc.* **2010**, *132*, 6312-6314.

- (15) Builes, S.; Vega L. F. Effect of Immobilized Amines on the Sorption Properties of Solid Materials: Impregnation versus Grafting. *Langmuir* **2013**, *29*, 199–206.
- (16) Zhao, Y.; Shen, Y.; Bai, L. Effect of Chemical Modification on Carbon Dioxide Adsorption Property of Mesoporous Silica. *J. Colloid Interface Sci.* **2012**, *379*, 94–100.
- (17) Bollini, P.; Didas, S. A.; Jones, W. Amine–Oxide Hybrid Materials for Acid Gas Separations. *J. Mater. Chem.* **2011**, *21*, 15,100–15,120.
- (18) Choi, S.; Drese, J. H.; Jones, C. W. Adsorbent Materials for Carbon Dioxide Capture from Large Anthropogenic Point Source. *ChemSusChem*, **2009**, *2*, 796–854.
- (19) Goepfert, A.; Meth, S.; Prakash, G. K. S.; Olah, G. A.; Nanostructured Silica as a Support for Regenerable High-Capacity Organoamine-Based CO₂ Sorbents. *Energy Environ. Sci.* **2010**, *3*, 1949–1960.
- (20) Wang, X.; Song, C. Temperature-Programmed Desorption of CO₂ from Polyethyleneimine–Loaded SBA-15 as Molecular Basket Sorbents. *Catal. Today* **2012**, *194*, 44–52.
- (21) Olah, G. A.; Goepfert, A.; Meth, S.; Prakash, G.K.; Nano-Structure Support Solid Regenerative Polyamine and Polyamine Polyol Absorbents for the Separation of Carbon Dioxide from Gas Mixture Including the Air. *U.S. Pat. Appl.* 2008 0293976, 2008.
- (22) Lin, Y.; Lin, H.; Wang, H.; Suo, Y.; Li, B.; Kong, C.; Chen, L. Enhanced selectivity CO₂ adsorption on polyamine/MIL-101 (Cr) composites. *J. Mater. Chem. A* **2014**, *2*, 14658-14665.

- (23) Xu, X.; Song, C.; Andrésen, J. M.; Miller, B. G.; Scaroni, A. W. Preparation and Characterization of Novel CO₂ “Molecular Basket” Adsorbents Based on Polymer-Modified Mesoporous Molecular Sieve MCM-41. *Microporous Mesoporous Mat.* **2003**, *62*, 29–45.
- (24) Xu, X.; Song, C.; Andresen, J. M.; Miller, B. G.; Scaroni, A. W. Novel Polyethyleneimine-Modified Mesoporous Molecular Sieve of MCM-41 Type as High-Capacity Adsorbent for CO₂ Capture. *Energy Fuels* **2002**, *16*, 1463–1469.
- (25) Sanz, R.; Calleja, G.; Arencibia, A.; Sanz-Pérez, E. S. CO₂ Adsorption on Branched Polyethyleneimine-Impregnated Mesoporous Silica SBA-15. *Appl. Surf. Sci.* **2012**, *256*, 5323–5328.
- (26) Sanz, R.; Calleja, G.; Arencibia, A.; Sanz-Pérez, E. S. Amino Functionalized Mesostructured SBA-15 Silica for CO₂ Capture: Exploring the Relation between the Adsorption Capacity and Distribution of Amino Groups by TEM. *Microporous Mesoporous Mat.* **2012**, *158*, 309–317.
- (27) Son, W. J.; Choi, J. S.; Ahn, W. S. Adsorptive Removal of Carbon Dioxide Using Polyethyleneimine-Loaded Mesoporous Silica Materials. *Microporous Mesoporous Mat.* **2008**, *113*, 31–40.
- (28) Witoon, T. Polyethyleneimine-loaded bimodal porous silica as low-cost and high-capacity sorbent for CO₂ capture. *Materials Chemistry and Physics* **2012**, *137*, 235-245.
- (29) Neimark, A. V.; Kheifets, L. I.; Fenelonov, V. B. Theory of Preparation of Supported Catalysts. *Ind. Eng. Chem. Prod. Res. Dev.* **1981**, *20*, 439–450.

- (30) Lee, S. Y.; Aris, R. The Distribution of Active Ingredients in Supported Catalysts Prepared by Impregnation. *Catal. Rev. Sci. Eng.* **1985**, *27*, 207–340.
- (31) Lekhal, A.; Glasser, B. J.; Khinast, J. G. Impact of Drying on the Catalyst Profile in Supported Impregnation Catalysts. *Chem. Eng. Sci.* **2001**, *56*, 4473–4487.
- (32) Jong, K. P. *Synthesis of Solid Catalysts*; WILEY-VCH Verlag GmbH & Co. KGaA: Weinheim, Germany, 2009.
- (33) Bourikas, K.; Kordulis, C.; Lycourghiotis, A. The Role of the Liquid–Solid Interface in the Preparation of Supported Catalysts. *Catal. Rev.-Sci. Eng.* **2006**, *48*, 363–444.
- (34) Maitra, A. M.; Cant, N. M.; Trimm, D. L. The Preparation of Tungsten Basted Catalysts by Impregnation of Alumina Pellets. *Appl. Catal.* **1986**, *27*, 9–19.
- (35) Zhu, B. Y.; Zhao, X.; Gu, T. Surface Solubilization. *J. Chem. Soc., Faraday Trans.1* **1988**, *84*, 3951–3960.
- (36) Stigter, B. D.; Williams, R. J.; Mysels, K. J. Micellar Self Diffusion of Sodium Lauryl Sulfate. *J. Phys. Chem.* **1955**, *59*, 330–335.
- (37) Sherrington, D. C. Preparation, Structure and Morphology of Polymer Supports. *Chem. Commun.* **1988**, *21*, 2275–2286.
- (38) Loganathan, S.; Tikmani, M.; Ghoshal, A. K. Novel Pore-Expanded MCM-41 for CO₂ Capture: Synthesis and Characterization. *Langmuir* **2013**, *29*, 3491–3499.
- (39) Wang, L. F.; Yang, R. T. Increasing Selective CO₂ Adsorption on Amine-Grafted SBA-15 by Increasing Silanol Density. *J. Phys. Chem. C* **2011**, *115*, 21,264–21,272.

- (40) Cervený, S.; Schwartz, G. A.; Otegui, J.; Colmenero, J.; Loichen, J.; Westermann, S. Dielectric Study of Hydration Water in Silica Nanoparticles. *J. Phys. Chem. C* **2012**, 116, 24,340–24,349.
- (41) Khdayr, N. H.; Ghanem, M. A. Metal–Organic–Silica Nanocomposites: Copper, Silver Nanoparticles–Ethylenediamine–Silica Gel and Their CO₂ Adsorption Behaviour. *J. Mater. Chem.* **2012**, 22, 12,032–12,038.
- (42) Al-Azzawi, O. M.; Hofmann, C. M.; Baker, G. A.; Baker, S. N. Nanosilica-Supported Polyethoxyamines as Low-cost, Reversible Carbon Dioxide Sorbents. *J. Colloid Interface Sci.* **2012**, 385, 154–159.
- (43) Yang, S.; Zhan, L.; Xu, X.; Wang, Y.; Ling, L.; Feng, X. Graphene-Based Porous Silica Sheets Impregnated with Polyethyleneimine for Superior CO₂ Capture. *Adv. Mater.* **2013**, 25, 2130–2134.
- (44) Peeters, A.; Ameloot, R.; Vos, D. E. D. Carbon Dioxide as a Reversible Amine-Protecting Agent in Selective Michael Additions and Acylations. *Green Chem.* **2013**, 15, 1550–1557.
- (45) Lee, D.; Jin, Y.; Jung, N.; Lee, J.; Lee, J.; Jeong, Y. S.; Jeon, S. Gravimetric Analysis of The Adsorption and Desorption of CO₂ on Amine-Functionalized Mesoporous Silica Mounted on a Microcantilever Array. *Environ. Sci. Technol.* **2011**, 45, 5704–5709.
- (46) Choi, S.; Gray, M. L.; Jones, C. W. Amine–Tethered Solid Adsorbents Coupling High Adsorption Capacity and Regenerability for CO₂ Capture from Ambient Air. *ChemSusChem* **2011**, 4, 628–635.

- (47) Cui, S.; Cheng, W.; Shen, X.; Fan, M.; Russell, A.; Wu, Z.; Yi, X. Mesoporous Amine-Modified SiO₂ Aerogel: A Potential CO₂ Sorbent. *Energy Environ. Sci.* **2011**, *4*, 2070–2074.
- (48) Srikanth, C. S.; Chuang, S. S. C. Infrared Study of sStrong and Weakly Adsorbed CO₂ on Fresh and Oxidatively Degraded Amine Sorbents. *J. Phys. Chem. C* **2013**, *117*, 9196–9205.
- (49) Wang, W.; Xiao, J.; Wei, X.; Ding, J.; Wang, X.; Song, C. Development of a New Clay Supported Polyethylenimine Composite for CO₂ Capture. *Appl. Energy* **2014**, *113*, 334–341.
- (50) Sayari, A.; Heydari-Gorji, A.; Yang, Y. CO₂-Induced Degradation of Amine-Containing Adsorbents: Reaction Products and Pathways. *J. Am. Chem. Soc.* **2012**, *134*, 13,834–13,842.

